Tracing the localization of 4f electrons: Angle-resolved photoemission on $YbCo_2Si_2$, the stable trivalent counterpart of the heavy-fermion $YbRh_2Si_2$

M. Güttler,[1,*] K. Kummer,[2] S. Patil,[1] M. Höppner,[3,1] A. Hannaske,[4] S. Danzenbächer,[1] M. Shi,[5] M. Radovic,[5] E. Rienks,[6] C. Laubschat,[1] C. Geibel,[4] and D. V. Vyalikh[1,7]

[1]*Institute of Solid State Physics, Dresden University of Technology, Zellescher Weg 16, D-01062 Dresden, Germany*
[2]*European Synchrotron Radiation Facility, 71, Avenue des Martyrs, Grenoble, France*
[3]*Max Planck Institute for Solid State Research, Heisenbergstrasse 1, D-70569 Stuttgart, Germany*
[4]*Max Planck Institute for Chemical Physics of Solids, Nöthnitzer Strasse 40, D-01187 Dresden, Germany*
[5]*Swiss Light Source, Paul Scherrer Institut, Aarebrücke, CH-5232 Villigen, Switzerland*
[6]*Helmholtz-Zentrum Berlin, BESSY II, Albert-Einstein-Strasse 15, D-12489 Berlin, Germany*
[7]*Department of Physics, St. Petersburg State University, St. Petersburg 198504, Russian Federation*

(Received 18 July 2014; published 20 November 2014)

$YbCo_2Si_2$ is considered to serve as a stable-valent, isoelectronic reference for the extensively studied heavy-fermion system $YbRh_2Si_2$ which is situated very close to an antiferromagnetic quantum critical point (QCP). The investigation of the Fermi surface (FS) topology of $YbCo_2Si_2$ and its comparison to $YbRh_2Si_2$ could help to unravel the strongly disputed nature of this quantum phase transition, whether it originates from a "local" or "itinerant" QCP. Here we study the electronic structure and FS of $YbCo_2Si_2$ by means of angle-resolved photoelectron spectroscopy (ARPES) and compare it to *ab initio* band structure calculations and FS modeling. Our approach allows the electronic structure at the surface and in the bulk to be disentangled. Identifying the bulk contribution, we demonstrate that $YbCo_2Si_2$ exhibits a "small" FS, confirming the formation of a "large" FS in $YbRh_2Si_2$. This favors an itinerant QCP, instead of the widely discussed local scenario. Our study demonstrates that ARPES is a reliable tool for the study of bulk electronic states in intermetallic Kondo lattice systems despite the complexity induced by their three-dimensional character and the presence of pronounced surface states.

DOI: 10.1103/PhysRevB.90.195138 PACS number(s): 79.60.−i, 71.27.+a, 71.70.Ch

Many exotic properties like high-temperature superconductivity, quantum criticality, or the breakdown of conventional metallic behavior observed in a large class of actively investigated materials are governed by strong electronic correlations [1–4]. At the heart of these phenomena lies the intricate crossover from localized corelike states to delocalized conduction states of a certain subset of electrons which leads to a complex entanglement of the many-particle system beyond a simple mean-field description.

The rare-earth intermetallic compounds $YbCo_2Si_2$ and $YbRh_2Si_2$ are Kondo lattice systems, in which strong correlations can emerge from the interaction between localized 4f states and extended valence states. An essential ingredient is the instability of the 4f shell of Yb: depending on the surrounding ligands, external pressure, or magnetic field, the Yb ions can exhibit different valence states, ranging from a trivalent magnetic configuration with one hole in the 4f shell to a nonmagnetic divalent configuration with a full 4f shell. In between, the quantum mechanical mixing of both states results in a paramagnetic intermediate valent state [5–7]. The transition from the magnetically ordered ground state to the paramagnetic one occurs usually at a quantum critical point (QCP) where the ordering temperature continuously decreases to $T = 0$ K. In some range on both sides of the QCP one observes strong electronic correlations between 4f and valence electrons, which, e.g., result in the formation of very heavy quasiparticles, hence the name heavy-fermion systems. With a Néel temperature T_N of merely 70 mK, $YbRh_2Si_2$ is very close to the border between the magnetically ordered and the paramagnetic states [8]. Therefore $YbRh_2Si_2$ has served as a model system for the study of quantum criticality in heavy-fermion systems [9,10]. Scanning tunneling spectroscopy and high-resolution angle-resolved photoelectron spectroscopy (ARPES) investigations were performed on this compound, giving detailed insight into its electronic structure [11–14]. The ARPES studies have revealed an enlarged Fermi surface (FS) at a temperature of 10 K [14] as expected when delocalized 4f degrees of freedom are part of the FS volume. However, this finding conflicts with the widely preferred "local" scenario for the QCP associated with the breakdown of Kondo singlets, which is based on the results of thermodynamic and transport measurements [15–17]. The other scenario debated to date assumes an "itinerant" QCP related to the formation of spin density waves (SDWs) [18]. Both scenarios should be reflected by a transition from a "large" to a "small" FS occurring either directly at the QCP or within the antiferromagnetic regime, respectively.

In order to ascertain the origin of this FS volume expansion, it is important to investigate the FS topology after suppressing the valence instability of the Yb 4f shell. This can be achieved by substituting Co for Rh in $YbRh_2Si_2$ [6]. $YbCo_2Si_2$ is known to be a stable trivalent Yb 4f system with $T_N = 1.7$ K [5,19]. Its Kondo temperature, which is a measure for the correlations between 4f and valence electrons, is at least a factor of 50 smaller than that in $YbRh_2Si_2$ [6]. $YbCo_2Si_2$ can therefore serve as a reference when studying the effects of valence instability on the FS topology within this family of materials.

Here we report the FS of $YbCo_2Si_2$ obtained by ARPES and compare it with results of *ab initio* band structure calculations that treat the 4f electrons as localized states. The correlation between the 4f and valence electrons is expected to be weak in this compound. Indeed, the good agreement between

*Corresponding author: guettler.monika@gmail.com

experimental data and theory points to a small FS that does not include the $4f$ degrees of freedom, providing a firm basis for the interpretation of our previous ARPES results on the strongly correlated homolog $YbRh_2Si_2$ [14]. The comparison indicates that in $YbRh_2Si_2$ the $4f$ degrees of freedom have entered the FS, which puts severe constraints on the nature of the QCP observed under a small magnetic field or negative chemical pressure.

ARPES experiments were performed at the SIS instrument of the Swiss Light Source and the 1^3 instrument at beamline UE112 PGM-2 at BESSY II, Berlin. Both instruments are equipped with a Scienta R4000 photoelectron energy analyzer. The SIS instrument has a six-axis CARVING manipulator with high angular precision which is ideally suited to efficiently map FSs at temperatures down to 10 K. The 1^3 instrument allows measurements at temperatures close to 1 K with ultrahigh energy resolution. The growth of the single crystals is described in Refs. [5,20]. All single crystals of $YbCo_2Si_2$ were cleaved in ultrahigh-vacuum conditions. As in $YbRh_2Si_2$, cleavage takes place between adjacent Si and Yb layers, where the interlayer bonding is relatively weak.

To model the band structure and FS of $YbCo_2Si_2$, we performed first-principles calculations based on density functional theory (DFT) in a general gradient approximation (GGA) using a full-potential local orbital basis [21]. The crystal-vacuum interface has been simulated by supercells containing symmetrical slabs of 31 atomic layers (with a total of seven Yb layers) for Si termination and 33 layers (with nine Yb layers) for Yb termination, allowing us to account for surface-related electronic states. The Yb $4f$ orbital has been removed from the variational basis set, applying a fixed unpolarized $4f^{13}$ configuration for trivalent Yb in the bulk and $4f^{14}$ for purely divalent Yb at the surface. We refer to this approach as the open-core approximation. Spin-orbit coupling has been omitted by choosing a spinless scalar-relativistic treatment. We will demonstrate that the electronic band structure of $YbCo_2Si_2$ as seen in ARPES can be satisfactorily modeled in this simple nonmagnetic approach with fully localized $4f$ electrons.

Figures 1(a) and 1(b) show ARPES-derived band maps for Si- and Yb-terminated surfaces of $YbCo_2Si_2$ along the $\overline{\Gamma}$-$\overline{M}$ direction of the surface Brillouin zone (BZ) taken at $T = 11$ K. Several spectral features can be identified for the Si-terminated crystal: (i) an intense linear dispersive band in the shape of a *Dirac cone* [22,23] labeled 1 at the $\overline{\Gamma}$ point with its apex 0.1 eV below the Fermi energy E_F, (ii) an electronlike band at the Fermi edge (2) as its counterpart, (iii) a bunch of bands forming a "waterfall"-type structure (3) cutting off halfway between $\overline{\Gamma}$ and $\overline{M}$ along with a similar structure (4) with much weaker intensity which runs parallel to the border of 3 and marks the edge of a bulk-projected gap around the $\overline{\mathrm{M}}$-point, and (iv) sharp electron- and holelike bands lying inside this gap (5). In the band map taken for Yb termination, the most prominent spectral features present at Si termination disappear, implying their surface-related origin as surface states or resonances due to their sensitivity to the surface boundary. In particular, the sharp bands around the $\overline{M}$ point have vanished. The prominent Dirac cone has faded as well, and only at higher binding energy (BE) may one detect a holelike band, which might be its trace shifted to higher BE.

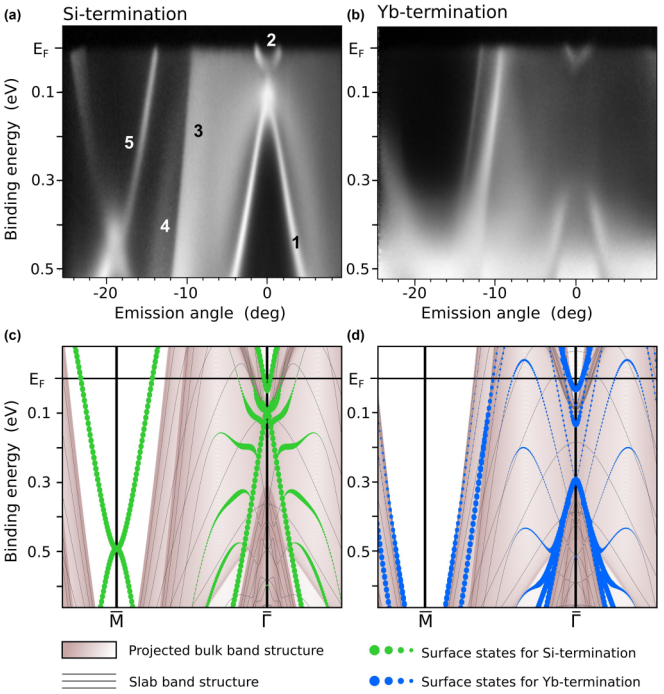

FIG. 1. (Color online) Comparison of measured and calculated band maps along $\overline{M}$-$\overline{\Gamma}$-$\overline{M}$. (a),(b) ARPES spectra taken at $T = 11$ K and 45 eV photon energy. (c),(d) Electronic band structures obtained from DFT-based calculations in the open-core approximation. Slab-derived surface states are indicated by green and blue dots for Si and Yb termination, respectively.

The electronlike band 2 at E_F remains visible with reduced intensity. As the waterfall-like band structures 3 and 4 persist at both terminations and hence are not subject to changes of the atomic surface configuration, they might be attributed to excitations from bulk-type bands.

To analyze the experimentally derived electronic band structure, DFT calculations in the open-core approximation have been performed using bulk and slab symmetries. Results for Si and Yb termination are depicted in Figs. 1(c) and 1(d), respectively. Wave functions with predominant localization within the surface region defined as the topmost four atomic layers are highlighted. The bulk band structure obtained from a pure bulk calculation is shown projected along $\boldsymbol{k}_z$ as shaded bands.

The calculated band structures are in good agreement with the ARPES results for both surface terminations. They clearly confirm the existence of a Shockley-type surface band around the $\overline{M}$ point within a gap of the projected bulk band structure at Si termination. As this band is missing in the Yb-terminated case, it serves as an unambiguous distinctive feature between the two terminations. Also, the clearly visible bands at the edge of the $\overline{M}$ gap for Yb termination seem well reproduced in the calculation. Due to their strong overlap with the projected bulk bands and almost the same dispersion they can be attributed to surface resonances reflecting the bulk band structure. Similarly, the holelike Dirac cone around the $\overline{\Gamma}$ point along with its electronlike counterpart seen sharply for Si termination are surface related. The waterfall bands 3 and 4 clearly seen in ARPES for Si termination, in contrast, are

nicely reproduced by the projected bulk band structure in the calculation, which confirms their bulk origin.

The fact that these simplified nonmagnetic band structure calculations with a fixed Yb 4f occupancy of 13.0 well reproduce all surface and bulk electron bands implies that the electronic structure near E_F can be mapped on a single-particle band structure and thus is adequately described in a one-electron picture. We therefore conclude that $YbCo_2Si_2$ does not reveal strong hybridization effects between 4f and conduction states such as mixed valency or heavy-fermion behavior, in perfect agreement with results from magnetic, thermodynamic, and transport measurements [5,6]. It thus provides a stable-valent reference system for isoelectronic heavy-fermion systems like $YbRh_2Si_2$ and $YbIr_2Si_2$. Note that the $YbCo_2Si_2$ spectra in Figs. 1(a) and 1(b) do not show flat 4f-derived quasiparticle bands at E_F, as were found in the isoelectronic Rh and Ir compounds [13,24]. This indicates a negligible admixture of the divalent $4f^{14}$ configuration to the ground state. An almost purely trivalent Yb state with a well-localized magnetic moment has also been found in magnetization and thermodynamic measurements. However, an increased Sommerfeld coefficient of $\gamma_0 = 0.13$ J mol K^{-2} along with a Kondo-type increase in electrical resistivity points to traces of hybridization between itinerant valence bands and localized Yb 4f states, in spite of predominant Ruderman-Kittel-Kasuya-Yosida (RKKY) exchange interaction in $YbCo_2Si_2$ [5].

Respective traces are also seen as a small bump at E_F in angle-integrated photoemission spectra [6]. The resonant x-ray emission spectroscopy (RXES) results shown in Fig. 2 further confirm some residual hybridization in $YbCo_2Si_2$. The sensitivity to small deviations from integer valency can be very high in Yb $L\alpha_1$ RXES [25]. Our data, taken at beamline ID16 of the ESRF, clearly show a very weak and temperature-dependent

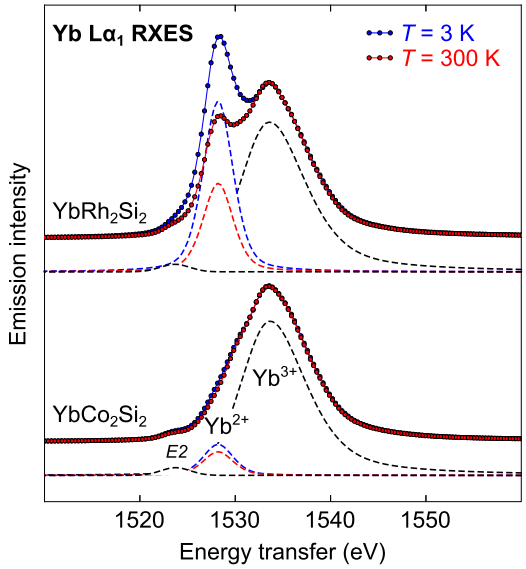

FIG. 2. (Color online) Resonant x-ray emission of $YbCo_2Si_2$ and $YbRh_2Si_2$ at low and room temperatures. The spectra were taken at constant emission energy in the Yb^{2+} resonance of the Yb L_3 absorption edge which strongly enhances Yb^{2+} contributions [25]. The dashed lines show the Yb^{2+} and Yb^{3+} components of the spectrum and the quadrupole transitions ($E2$).

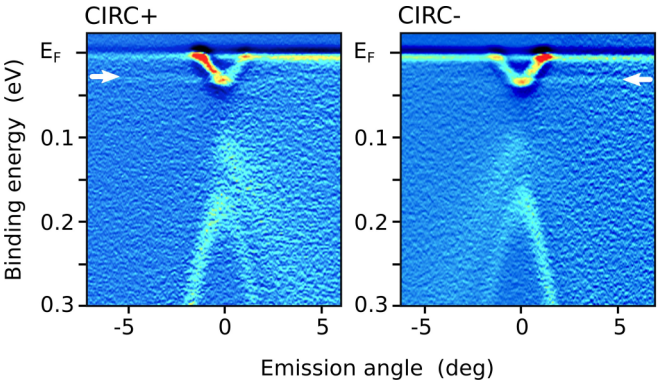

FIG. 3. (Color online) ARPES fine structure band maps taken along $\overline{\Gamma}$ and $\overline{M}$ at ~1 K temperature with circularly right (CIRC+) and left (CIRC−) polarized photons of 45 eV energy. Numerical application of a high-pass filter amplifies the spectral intensity of the otherwise extremely weak 4f-derived bands indicated by arrows.

Yb^{2+} fraction in $YbCo_2Si_2$. We therefore expected to find some signatures of partial hybridization in ARPES spectra at enhanced resolution. Figure 3 shows the fine electronic structure near E_F taken at BESSY II at $T \sim 1$ K. The ARPES band maps were obtained with circularly polarized light, allowing geometric dichroism to be observed [13]. A numerical high-pass filter was applied to the spectra to enhance flat spectral features. In each of the two spectra one detects a weak flat band at 30 meV BE appearing only on one side with respect to the BZ center. The polarization dependence of the ARPES intensity indicates an anisotropic orbital symmetry of the initial state. The extreme flatness and closeness of the observed band to E_F as well as the anisotropy are strongly reminiscent of the 4f-derived heavy-quasiparticle bands observed in $YbRh_2Si_2$ and $YbIr_2Si_2$ [13,24] and can therefore be assigned to Yb 4f excitations. These excitations arise due to a tiny $4f^{14}$ contribution to the ground-state wave function. Their presence thus confirms some residual hybridization between the Yb 4f shell and itinerant states in $YbCo_2Si_2$. As in the isoelectronic Rh and Ir compounds, the fine structure of the detected 4f emission in $YbCo_2Si_2$ can be attributed to a splitting of the $^2F_{7/2}$ final state in the crystalline electric field. The latter was earlier studied by means of inelastic neutron scattering, suggesting that three excited Kramers doublets are separated from the ground-state doublet by 4, 12.5, and 30.5 meV [26]. The energy of the topmost excited doublet at 30.5 meV matches well the energy of the 4f band at 30 ± 2 meV found by ARPES (Fig. 3). This confirmation of neutron scattering results further supports the derivation presented in Ref. [5] leading to a Γ_7 irreducible representation of the ground state in $YbCo_2Si_2$. The ARPES results agree with the picture of a tiny residual Kondo-type resonance at E_F in $YbCo_2Si_2$ which splits in the crystalline electric field.

In Figs. 4(a) and 4(b) the ARPES-derived FSs of $YbCo_2Si_2$ measured at 11 K on Si- and Yb-terminated crystals are compared to calculated FSs. The simulated maps have been obtained similarly to the previously discussed band structures by superposition of surface-related states and projected bulk bands. In general, the experimental FSs for both surface terminations look rather similar and are in good agreement

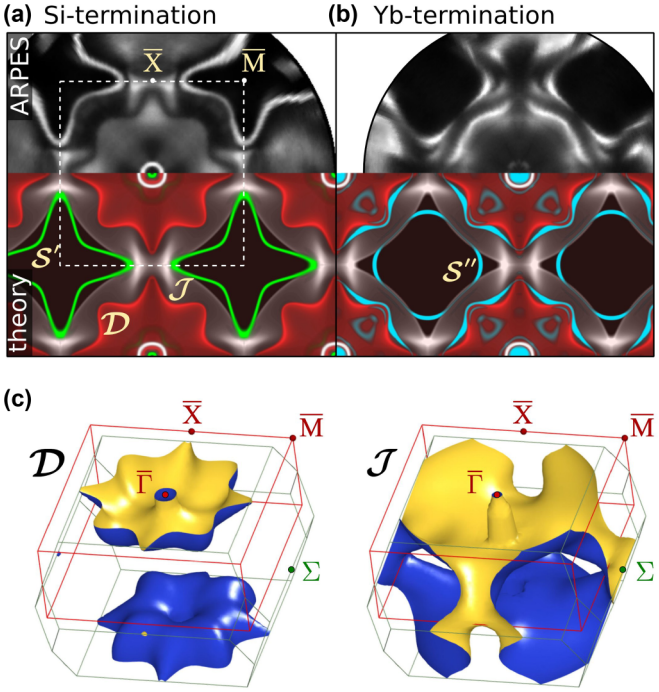

FIG. 4. (Color online) (a),(b) Comparison of experimental and calculated FSs for (a) Si and (b) Yb surface termination. The upper gray scale images show FSs obtained by ARPES using a photon energy of 45 eV at 11 K temperature. The colored FSs in the lower panels were derived from band structure calculations employing the open-core approach. Bulk FS sheets are labeled $\mathcal{D}$ (red) and $\mathcal{J}$ (gray). Surface states obtained from the slab supercells are labeled $\mathcal{S}'$ (green) and $\mathcal{S}''$ (cyan) for Si and Yb termination, respectively. The first surface BZ is indicated by a dotted square. (c) Three-dimensional (3D) representation of the bulk FS sheets $\mathcal{D}$ and $\mathcal{J}$. The $\boldsymbol{k}$ space used for projection along $\boldsymbol{k}_z$ is designated by a red cuboid. The 2D surface BZ is indicated by the red square on top of the 3D BZ. Blue (yellow) denotes the inner (outer) FS face.

with the open-core calculation. The differences between both terminations can be consistently attributed to surface states and resonances. For instance, a sharp diamond-shaped feature lies inside the bulk-projected $\overline{M}$ gap in the Si-terminated FS, which is clearly missing in the Yb-terminated case. It corresponds to the Shockley-type surface band 5 in Fig. 1. A similar Shockley state on the Si-terminated surface of $EuRh_2Si_2$ has recently been shown to undergo a large spin splitting at low temperature due to exchange coupling to the ferromagnetically ordered Eu layer beneath the surface [27]. Such a splitting does not seem to occur in $YbCo_2Si_2$, probably due to the rather low ordering temperature of $T_N = 1.7$ K, the much smaller ordering moment of $1.4\mu_B$ compared to $7\mu_B$ in $EuRh_2Si_2$ and a likely more complicated magnetic order.[1]

The bulk electronic structure at E_F is dominated by two FS sheets $\mathcal{D}$ and $\mathcal{J}$ depicted in the 3D $\boldsymbol{k}$ space in Fig. 4(c).

[1]Neutron scattering studies have revealed an incommensurate structure between $T_{N_1} = 1.7$ K and $T_{N_2} = 0.9$ K and a commensurate one below T_{N_2}, with propagation vectors $Q_{AF_1} = (\frac{1}{4}, 0.08, 1)$ and $Q_{AF_2} = (\frac{1}{4}, \frac{1}{4}, 1)$, respectively [28,29].

Additionally, a small cylindrical electron pocket $\mathcal{P}$ centered at Γ, which is not explicitly shown here, arises in our calculations. We found that its energy position sensitively depends on the z_{Si} coordinate of the Si atoms, as has also been shown for $LuRh_2Si_2$ [30]. In our calculations, the "pillbox" $\mathcal{P}$ is part of the FS for $z_{Si} \lesssim 0.379$. The electron pocket can be detected in both the Yb-terminated ARPES band map in Fig. 1(b), where the bottom of the band amounts to ~40 meV, and the respective FS in Fig. 4(b) as a ring with very weak intensity around $\overline{\Gamma}$. However, a surface origin of this band cannot be ruled out, as the band structure calculations suggest the existence of an almost degenerate surface state. Such a band could not be directly observed in $YbRh_2Si_2$. In the Rh compound, a slight bending of the $4f$-derived quasiparticle bands at E_F, however, points to the existence of a similar electronlike band slightly above E_F [13].

The FS sheet $\mathcal{J}$—the "jungle gym"—is largely interconnected with neighboring BZs. The "arms" reaching towards the Σ points contain larger parts with weak $\boldsymbol{k}_z$ dispersion. They show up in the experimental and simulated 2D FSs as intense features around $\overline{X}$, which separate the FS sheets labeled $\mathcal{D}$ from neighboring surface Brillouin zones. In $YbRh_2Si_2$, this $\mathcal{J}$ sheet is rather blurred and hardly traceable in the ARPES-derived FS map (see Ref. [14]), probably due to $4f$-induced renormalization.

The main feature of interest, however, is the square, "doughnut"-shaped bulk FS sheet $\mathcal{D}$. The topology of this sheet plays a significant role in the disclosure of the nature of the antiferromagnetic quantum phase transition in $YbRh_2Si_2$. This FS sheet forms disjoint hole pockets in the $\boldsymbol{k}$ space and is ideally suited to track changes of the FS volume. In $YbCo_2Si_2$ the doughnut lies entirely inside the first BZ. Its size and topology perfectly match the theoretical FS sheet obtained in the open-core approximation which neglects any hybridization between the localized $4f$ shell and itinerant states. Thus the FS of $YbCo_2Si_2$ can be identified as a small FS which does not include degrees of freedom of the Yb $4f$ hole. The ARPES-derived FS of $YbRh_2Si_2$ shows a similar topology, but in contrast to the Co system the doughnut is enlarged and reaches into the neighboring BZ by open necks at the $\overline{X}$ point [14]. With the FS of $YbCo_2Si_2$ as reference for the small FS, the enlargement of the doughnut in $YbRh_2Si_2$ compared to the unhybridized case is clearly confirmed and can be attributed to the formation of a large FS including the Yb $4f$ hole.

In summary, we studied the electronic properties of $YbCo_2Si_2$, which is isoelectronic to the quantum critical heavy-fermion system $YbRh_2Si_2$, by means of ARPES. Band structure calculations in the framework of DFT with the GGA were performed to analyze and interpret the experimental results. The ARPES spectra reveal many well-resolved structures, which are in excellent agreement with predictions of the DFT calculations. This demonstrates that ARPES is a reliable tool for the study of electronic states in intermetallic Kondo lattice systems. Although tiny signatures of residual Yb $4f$ spectral weight in the vicinity of the Fermi edge are observed, these f contributions are too weak to significantly affect the dispersion of the itinerant electron bands close to E_F. From the remarkable agreement between the simplified band structure calculation and the ARPES-derived FS we conclude

that no f spectral weight is transferred to the FS. This is in agreement with previous experimental findings, which found the Yb ion in $YbCo_2Si_2$ to be stable trivalent with no signatures of heavy-fermion behavior. The observed FS sheets can be interpreted in terms of a small FS, which does not include f-hole degrees of freedom, thus yielding a clear reference for the interpretation of the FS observed in $YbRh_2Si_2$ by means of ARPES. The differing FS topology of $YbRh_2Si_2$ compared to its Co counterpart can be attributed to the formation of a large FS counting the 4f hole. This observation of the large FS in ARPES at zero external field in $YbRh_2Si_2$ contradicts the interpretation of the so-called T^* line to be a transition from the large to the small FS upon decreasing the field proposed within the local QCP scenario. Under the assumption that the volume enclosed by this FS does not decrease upon lowering the temperature from 1 K, the lowest accessible T in ARPES, to below the Néel temperature $T_N = 70$ mK, our results would imply the QCP in $YbRh_2Si_2$ to be of SDW type, with the change from a large to a small FS occurring somewhere in between the Rh and the Co compounds, i.e., within the magnetically ordered regime.

This work was supported by the DFG (Grants No. VY64/1-3 and No. GE602/2-3).

[1] P. A. Lee, N. Nagaosa, and X.-G. Wen, Rev. Mod. Phys. **78**, 17 (2006).
[2] Q. Si and F. Steglich, Science **329**, 1161 (2010).
[3] P. Gegenwart, Q. Si, and F. Steglich, Nat. Phys. **4**, 186 (2008).
[4] G. R. Stewart, Rev. Mod. Phys. **73**, 797 (2001); **78**, 743 (2006).
[5] C. Klingner, C. Krellner, M. Brando, C. Geibel, and F. Steglich, New J. Phys. **13**, 083024 (2011).
[6] C. Klingner, C. Krellner, M. Brando, C. Geibel, F. Steglich, D. V. Vyalikh, K. Kummer, S. Danzenbächer, S. L. Molodtsov, C. Laubschat, T. Kinoshita, Y. Kato, and T. Muro, Phys. Rev. B **83**, 144405 (2011).
[7] O. Trovarelli, C. Geibel, S. Mederle, C. Langhammer, F. M. Grosche, P. Gegenwart, M. Lang, G. Sparn, and F. Steglich, Phys. Rev. Lett. **85**, 626 (2000).
[8] P. Gegenwart, J. Custers, C. Geibel, K. Neumaier, T. Tayama, K. Tenya, O. Trovarelli, and F. Steglich, Phys Rev Lett **89**, 056402 (2002).
[9] S. Paschen, T. Luhmann, S. Wirth, P. Gegenwart, O. Trovarelli, C. Geibel, F. Steglich, P. Coleman, and Q. Si, Nature (London) **432**, 881 (2004).
[10] S. Friedemann, T. Westerkamp, M. Brando, N. Oeschler, S. Wirth, P. Gegenwart, C. Krellner, C. Geibel, and F. Steglich, Nat. Phys. **5**, 465 (2009).
[11] S. Ernst, S. Kirchner, C. Krellner, C. Geibel, G. Zwicknagl, F. Steglich, and S. Wirth, Nature (London) **474**, 362 (2011).
[12] D. V. Vyalikh, S. Danzenbächer, Y. Kucherenko, C. Krellner, C. Geibel, C. Laubschat, M. Shi, L. Patthey, R. Follath, and S. L. Molodtsov, Phys. Rev. Lett. **103**, 137601 (2009).
[13] D. V. Vyalikh, S. Danzenbächer, Yu. Kucherenko, K. Kummer, C. Krellner, C. Geibel, M. G. Holder, T. K. Kim, C. Laubschat, M. Shi, L. Patthey, R. Follath, and S. L. Molodtsov, Phys. Rev. Lett. **105**, 237601 (2010).
[14] S. Danzenbächer, D. V. Vyalikh, K. Kummer, C. Krellner, M. Holder, M. Höppner, Yu. Kucherenko, C. Geibel, M. Shi, L. Patthey, S. L. Molodtsov, and C. Laubschat, Phys. Rev. Lett. **107**, 267601 (2011).
[15] P. Coleman, C. Pépin, Q. Si, and R. Ramazashvili, J. Phys.: Condens. Matter **13**, R723 (2001).
[16] Q. Si, S. Rabello, K. Ingersent, and J. L. Smith, Nature (London) **413**, 804 (2001).
[17] J. Custers, P. Gegenwart, H. Wilhelm, K. Neumaier, Y. Tokiwa, O. Trovarelli, C. Geibel, F. Steglich, C. Pépin, and P. Coleman, Nature (London) **424**, 524 (2003).
[18] E. Abrahams and P. Wölfle, Proc. Natl. Acad. Sci. USA **109**, 3238 (2012).
[19] J. A. Hodges, Europhys. Lett. **4**, 749 (1987).
[20] C. Krellner, S. Taube, T. Westerkamp, Z. Hossain, and C. Geibel, Philos. Mag. **92**, 2508 (2012).
[21] K. Koepernik and H. Eschrig, Phys. Rev. B **59**, 1743 (1999).
[22] S. N. Molotkov, JETP Lett. **90**, 339 (2009).
[23] M. Höppner, S. Seiro, A. Chikina, A. Fedorov, M. Güttler, S. Danzenbächer, A. Generalov, K. Kummer, S. Patil, S. L. Molodtsov, Y. Kucherenko, C. Geibel, V. N. Strocov, M. Shi, M. Radovic, T. Schmitt, C. Laubschat, and D. V. Vyalikh, Nat. Commun. **4**, 1646 (2013).
[24] S. Patil, K. Kummer, A. Hannaske, C. Krellner, M. Kuhnt, S. Danzenbächer, C. Laubschat, C. Geibel, and D. Vyalikh, JPS Conf. Proc. **3**, 011001 (2014).
[25] K. Kummer, Y. Kucherenko, S. Danzenbächer, C. Krellner, C. Geibel, M. G. Holder, L. V. Bekenov, T. Muro, Y. Kato, T. Kinoshita, S. Huotari, L. Simonelli, S. L. Molodtsov, C. Laubschat, and D. V. Vyalikh, Phys. Rev. B **84**, 245114 (2011).
[26] E. A. Goremychkin and R. Osborn, J. Appl. Phys. **87**, 6818 (2000).
[27] A. Chikina, M. Höppner, S. Seiro, K. Kummer, S. Danzenbächer, S. Patil, A. Generalov, M. Güttler, Yu. Kucherenko, E. V. Chulkov, Yu. M. Koroteev, K. Koepernik, C. Geibel, M. Shi, M. Radovic, C. Laubschat, and D. V. Vyalikh, Nat. Commun. **5**, 3171 (2014).
[28] K. Kaneko, O. Stockert, N. Mufti, K. Kiefer, C. Klingner, Cornelius Krellner, C. Geibel, and F. Steglich, J. Phys.: Conf. Ser. **200**, 032031 (2010).
[29] A. Hannaske, O. Stockert, C. Klingner, C. Krellner, S. Matas, L. Pedrero, M. Brando, C. Geibel, and F. Steglich, Phys. Status Solidi B **250**, 476 (2013).
[30] S. Friedemann, S. K. Goh, P. M. C. Rourke, P. Reiss, M. L. Sutherland, F. M. Grosche, G. Zwicknagl, and Z. Fisk, New J. Phys. **15**, 093014 (2013).